

# Linear Time-Frequency Analysis in High Resolution SAR Images and Applications

Ammar Mian<sup>1,2</sup>, Jean-Philippe Ovarlez<sup>1,3</sup>, Guillaume Ginolhac<sup>2</sup> and  
Abdourrahmane M. Atto<sup>2</sup>

<sup>1</sup>French Aerospace Lab, ONERA DEMR/TSI, France

<sup>2</sup>LISTIC, Université de Savoie Mont-Blanc, F-74944, Annecy le Vieux, France

<sup>3</sup>SONDRA CentraleSupélec, France

Peyresq 2017



# Contents

## 1 Background on SAR and Radar Imaging

- Principle of SAR Acquisition
- Multi-Channel SAR Images
- Mono-Channel SAR Images

## 2 Time-Frequency distributions for SAR Imaging

- Highlighting the Spectral and Angular Behaviours of the Scatterers
- Time-Frequency distributions for analysing these behaviours
- In practice
- From Mono-Channel to Multi-Channel SAR Image

## 3 Applications

- Data Model
- Target Detection
- Change Detection

## 4 Conclusion and perspectives

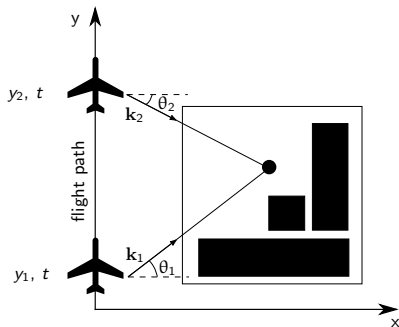


**Figure:** SAR acquisition geometry. A reflector is viewed at two different angles of illumination  $\theta_1$  and  $\theta_2$ .

Bright points model:

$$I(\mathbf{r}) = \sum_k h_k \delta(\mathbf{r} - \mathbf{r}_k)$$

$\mathbf{r} = [x, y]^T$ : scatterer position.  
 $h_k$ : Backscattering coefficient.

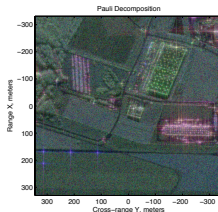
SAR image construction:

$$I(\mathbf{r}) = \int_{\mathcal{D}} H(\mathbf{k}) \exp(2i\pi \mathbf{k}^T \mathbf{r}) d\mathbf{k},$$

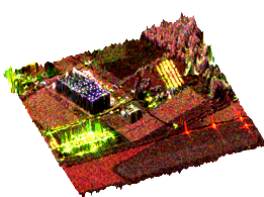
$\mathbf{k} = [k \cos(\theta), k \sin(\theta)]$ : wave vector.  
 $H$ : backscattering coefficient for each  $\mathbf{k}$ .  
 $\mathcal{D}$ : frequency and angular support of  $H$ .

Multi-channel SAR images automatically propose a diversity through:

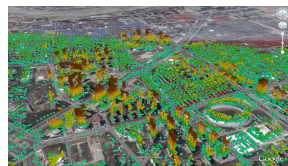
- polarimetric channels (POLSAR), interferometric channels (INSAR), polarimetric and interferometric channels (POLINSAR),
- multi-temporal, multi-passes SAR Image, etc.



EM behavior of the terrain  
in POLSAR images



Estimation of the height  
in POLINSAR images

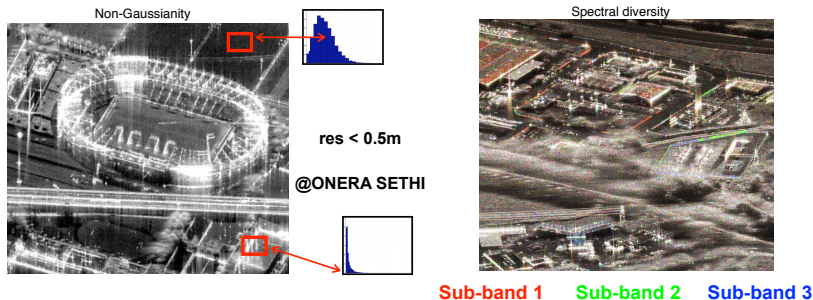


Analysis of the structures displacement in  
Shanghai with multi-temporal SAR images  
(@Telespazio)

Almost all the conventional techniques of detection, parameters estimation, speckle filtering techniques, classification in multi-channel SAR images (e.g. polarimetric covariance matrix, interferometric coherency matrix) are based on the **multivariate statistic**.

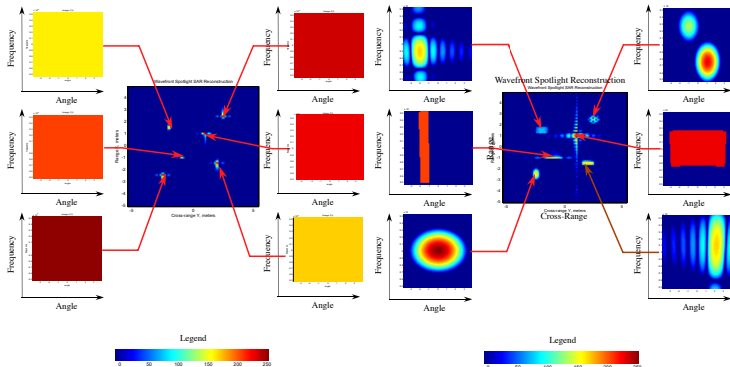
For mono-channel SAR Images, each pixel of the spatial image is **only** characterized by a complex amplitude and we don't have directly access any diversity. Moreover,

- very high resolution SAR images are more and more complex, detailed, heterogeneous,
- the spatial statistic of SAR images may be **not at all Gaussian** !
- SAR pixels may be **dispersive** (or colored) and **anisotropic** [Duquenoy et al., 2010].



### Challenging Problems

- How to retrieve, how to exploit this diversity (dispersive and anisotropic information) from mono-channel SAR image ?
- How to derive Multivariate Adaptive Detectors on a mono-channel complex SAR image ?



- An isotropic and white scatterer is mainly located on a pixel of SAR image,
  - An anisotropic and colored scatterer may naturally spread out in spatial domain !

Time-Frequency Distributions are generally devoted to non-stationary time signals analysis (e.g. spectral components varying with time). They can be easily extended in 2D.

**Key idea:** In the context of SAR Imaging, Time-Frequency Analysis allows:

- to highlight the coloration and anisotropy properties of monodimensional SAR scatterers,
- to characterize each pixel of the complex SAR image with a vector of information related to angular or/and frequency behaviors.

LTFD analysis and the physical group theory (Heisenberg or affine group) allow to construct **hyperimages** [J. and P. Bertrand, 1991, J.P. Ovarlez, 2003] through:

$$\tilde{I}(\mathbf{r}_0, \mathbf{k}_0) = \langle H(\cdot), \Psi_{\mathbf{r}_0, \mathbf{k}_0}(\cdot) \rangle = \int_{\mathcal{D}_{\mathbf{k}}} H(\mathbf{k}) \Psi_{\mathbf{r}_0, \mathbf{k}_0}^*(\mathbf{k}) d\mathbf{k},$$

where  $\Psi_{\mathbf{r}_0, \mathbf{k}_0}(\mathbf{k})$  is a family of wavelet bases (Gabor, wavelet) generated from a mother wavelet  $\phi(f, \theta)$  through the chosen physical group of transformation (translations, scale in frequency, etc.) and where  $\mathcal{D}_{\mathbf{k}}$  is the spectral/angular support of the wavelet  $\Psi$ .

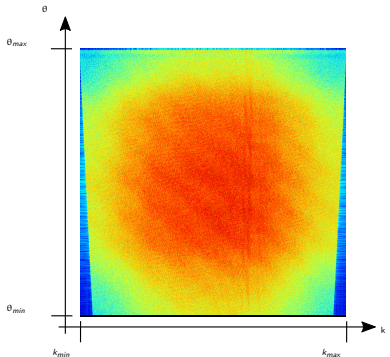


Figure:  $H(\mathbf{k})$

We want to decompose the  $(k, \theta)$  space in  $N_k$  sub-bans and  $N_\theta$  sub-looks without losing information.  
 $\kappa = k_{\max} - k_{\min}$ ,  $\Theta = \theta_{\max} - \theta_{\min}$ .  
 We can define the function  $\phi_{I,m}(k, \theta)$ :

$$\phi_{I,m}(k, \theta) = \begin{cases} 1 & \text{if } (k, \theta) \in \Delta_{I,m} \\ 0 & \text{otherwise} \end{cases}$$

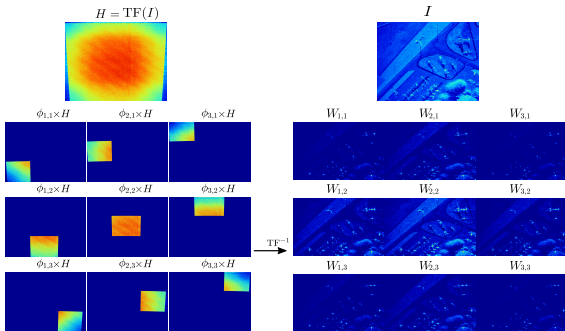
with

$$\begin{aligned} \Delta_{I,m} = & \left[ k_{\min} + \frac{(I-1)\kappa}{N_k}, k_{\min} + \frac{I\kappa}{N_k} \right] \\ & \cup \left[ \theta_{\min} + \frac{(m-1)\Theta}{N_\theta}, \theta_{\min} + \frac{m\Theta}{N_\theta} \right]. \end{aligned}$$

Decomposition:

$$W_{I,m}(\mathbf{r}) = \int_0^{2\pi} d\theta \int_0^{+\infty} k H(k, \theta) \phi_{I,m}(k, \theta) e^{+j2\pi\mathbf{k}^T \mathbf{r}} dk$$

Example of  $N_f = 3$  sub-bands and  $N_\theta = 3$  sub-looks image decomposition:



### Exploitation of the diversity

Each pixel  $i$  of the mono-channel SAR image can now be characterized by a  $N$ -vector

$\mathbf{x}_i = [W_{1,1}^i, \dots, W_{N_f, N_\theta}^i]^T$  of information ( $N = N_f N_\theta$ ) related to **dispersion** in frequency domain and **anisotropy** in angular domain. Which multivariate statistic can characterize the vector  $\mathbf{x}_i$  ?

To model the distribution of the vector  $\mathbf{x}_i$ , we can use:

- Complex Circular Gaussian with zero mean:

$$p(\mathbf{x}_i) = \pi^{-N} |\Sigma|^{-1} \exp\left(-\mathbf{x}_i^H \Sigma^{-1} \mathbf{x}_i\right)$$

But, Gaussian statistics are not really adapted to high resolutions SAR images ! Need to extend the Gaussian hypothesis.

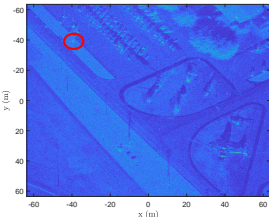
- Complex Elliptically Symmetric (CES): [E. Ollila, 2012]

$$g_{\mathbf{x}_i}(\mathbf{x}_i) = \pi^{-N} |\Sigma|^{-1} h_{\mathbf{x}_i}\left(\mathbf{x}_i^H \Sigma^{-1} \mathbf{x}_i\right),$$

where  $h_{\mathbf{x}_i} : [0, \infty) \rightarrow [0, \infty)$  is the density generator,  $\Sigma$  is the scatter matrix.

- Large class of distributions closed under affine transformations: Gaussian ( $h_{\mathbf{x}}(u) = \exp(-u)$ ), SIRV, MGDD ( $h_{\mathbf{x}_i}(u) = \exp(-u^\alpha)$ ), etc.,
- Stochastic representation theorem:  $\mathbf{x}_i =_d \mathcal{R}_i \mathbf{A}_i \mathbf{u}_i$ , where  $\mathcal{R} \geq 0$ , independent of  $\mathbf{u}$  and  $\Sigma = \mathbf{A} \mathbf{A}^H$ ,

- In our approach,  $\Sigma$  characterizes locally the correlation structure existing within the frequency and angular channels,
- The texture random variable  $\mathcal{R}_i$  is modeling the power variation of each vector  $\mathbf{x}_i$  from pixels to pixels and then characterizes the spatial power heterogeneity of the SAR image.



### Gaussian Case

Two-step GLRT AMF test [F. C. Robey *et al.*, 1992]

$$\Lambda_{AMF}(\mathbf{x}) = \frac{\left| \mathbf{p}^H \hat{\Sigma}_{SCM}^{-1} \mathbf{x} \right|^2}{\mathbf{p}^H \hat{\Sigma}_{SCM}^{-1} \mathbf{p}} \stackrel{H_1}{\gtrless} \stackrel{H_0}{\lessgtr} \lambda_{AMF}.$$

$$\text{With } \hat{\Sigma}_{SCM} = \frac{1}{K} \sum_{i=1}^K \mathbf{x}_i \mathbf{x}_i^H$$

$\Lambda_{AMF}$  is CFAR w.r.t  $\Sigma$

$\Lambda_{ANMF}$  is CFAR w.r.t  $Sigma$  and  $\mathcal{R}$

We search a target with a known steering vector  $\mathbf{p} \in \mathbb{C}^{N=N_k \times N_\theta}$  on a SAR Image.

$$\begin{cases} H_0 : \mathbf{x}_i = \mathbf{b}_i & \& \mathbf{x}_k = \mathbf{b}_k, k = 1, \dots, K \\ H_1 : \mathbf{x}_i = \alpha \mathbf{p} + \mathbf{b}_i & \& \mathbf{x}_k = \mathbf{b}_k, k = 1, \dots, K \end{cases}$$

$\mathbf{b}$  is either Gaussian or CES noise.  $\alpha \in \mathbb{C}$  is an unknown attenuation factor.

### CES Case

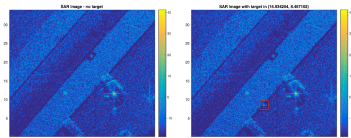
Two-step GLRT ANMF [E. Conte, 1995, S. Kraut/L. Scharf, 1999]

$$\Lambda_{ANMF}(\mathbf{x}) = \frac{\left| \mathbf{p}^H \hat{\Sigma}_{TE}^{-1} \mathbf{x} \right|^2}{\left| \mathbf{x}^H \hat{\Sigma}_{TE}^{-1} \mathbf{x} \right| \left| \mathbf{p}^H \hat{\Sigma}_{TE}^{-1} \mathbf{p} \right|} \stackrel{H_1}{\gtrless} \stackrel{H_0}{\lessgtr} \lambda_{ANMF},$$

where  $\hat{\Sigma}_{TE}$  stands for Tyler's estimator [D. Tyler, 1997, F. Gini, 2002, F. Pascal, 2008]:

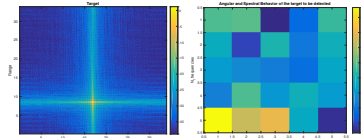
$$\hat{\Sigma}_{TE} = \frac{N}{K} \sum_{k=1}^K \frac{\mathbf{x}_k \mathbf{x}_k^H}{\mathbf{x}_k^H \hat{\Sigma}_{TE}^{-1} \mathbf{x}_k},$$

### Dataset from SANDIA National Laboratories



Left: Original SAR Image without target. Right:  
SAR image with specific embedded target.

### Artificial embedded target

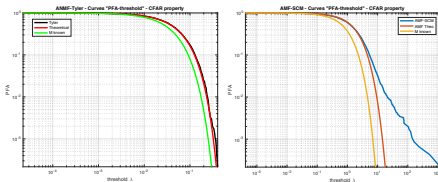


Left: SAR Image of the target. Right: True target response  $p$  in angular and spectral spaces ( $N_\theta = 5$  sub-looks,  $N_f = 5$  sub-bands).

### Analysis of Performance

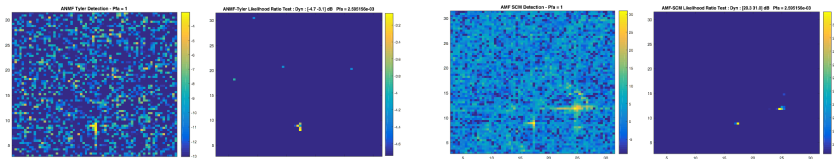
- Evaluation the CFAR property of the AMF and ANMF detectors,
- Comparison of the target detection performance between AMF and ANMF.

## Perfect PFA regulation with ANMF-TE but poor PFA regulation for AMF-SCM



Left: FA Regulation with ANMF-Tyler. Right: FA Regulation with AMF-SCM.  $N_\theta = 5$ ,  $N_f = 5$ ,  $K = 88$ .

## Better target detection for ANMF-TE



Left: ANMF-TE detection test,  $P_{fa} = 1$ . Right: ANMF-TE detection test,  $P_{fa} = 2.6 \cdot 10^{-3}$ .

Left: Full AMF-SCM detection test,  $P_{fa} = 1$ . Right: AMF-SCM detection test,  $P_{fa} = 2.6 \cdot 10^{-3}$ .

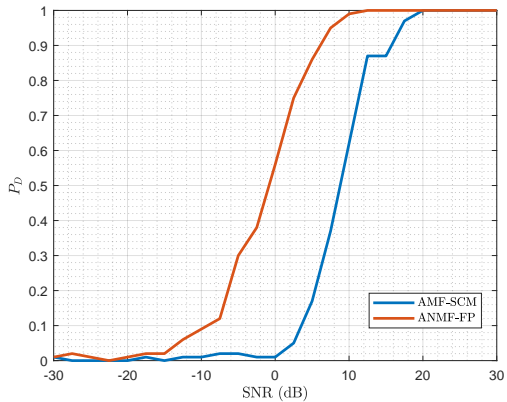
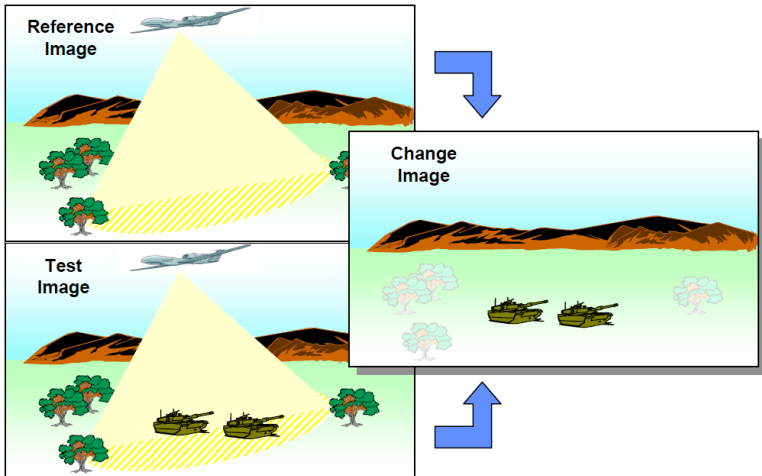


**Figure:**  $P_D = f(\text{SNR})$  computed on 100 Monte-Carlo trials ( $P_{FA} = 10^{-3}$ ,  $N_k = N_\theta = 5$ ,  $K = 105$ , random position of the target and random steering vector)

## Change Detection:



Developed for Polarimetry in [Novak, 2005]. Extension to spectro-angular features:

## Data Model

$$\begin{cases} \mathbf{I} = [\mathbf{i}_1, \mathbf{i}_2, \dots, \mathbf{i}_M] \in \mathbb{C}^{N \times M} \\ \mathbf{J} = [\mathbf{j}_1, \mathbf{j}_2, \dots, \mathbf{j}_M] \in \mathbb{C}^{N \times M} \end{cases} \quad \text{with } \forall k, \mathbf{i}_k \sim \mathcal{CN}(\mathbf{0}_p, \mathbf{C}_i) \text{ and } \mathbf{j}_k \sim \mathcal{CN}(\mathbf{0}_p, \mathbf{C}_j)$$

## Detection Test

$$\begin{cases} H_0 : \mathbf{C}_i = \mathbf{C}_j = \mathbf{C} \\ H_1 : \mathbf{C}_i \neq \mathbf{C}_j \end{cases}$$

$$\text{Test is } \hat{\lambda}_{\text{multi}} = \frac{|\hat{\mathbf{C}}|^{2M}}{|\hat{\mathbf{C}}_i|^M |\hat{\mathbf{C}}_j|^M} \stackrel{H_1}{\gtrless} \lambda$$

with:

$$\begin{aligned} \hat{\mathbf{C}} &= \frac{1}{2M} \sum_{k=1}^M \mathbf{i}_k \mathbf{i}_k^H + \mathbf{j}_k \mathbf{j}_k^H, \\ \hat{\mathbf{C}}_i &= \frac{1}{M} \sum_{k=1}^M \mathbf{i}_k \mathbf{i}_k^H, \\ \hat{\mathbf{C}} &= \frac{1}{M} \sum_{k=1}^M \mathbf{j}_k \mathbf{j}_k^H. \end{aligned}$$

## Multivariate Case ( $M = 1$ )

$$\hat{\lambda}_{\text{mono}} = \frac{\left( \sum_{k=1}^K |i_k|^2 + \sum_{k=1}^K |j_k|^2 \right)^2}{\sum_{k=1}^K |i_k|^2 \sum_{k=1}^K |j_k|^2} \stackrel{H_1}{\gtrless} \lambda$$

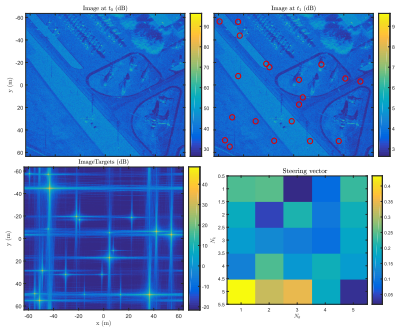


**Figure:** Example of change generated (SNR: random between  $[0; 30]$  dB, position: random on the image). Top-Left: Image **I**. Top-Right: Image **J** (changes are circled in red). Bottom-Left: Image of targets. Bottom-Right: Steering vector of one target.

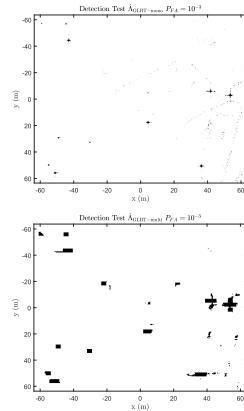


**Figure:** Detection test at  $P_{FA} = 10^{-3}$ .  
 Top:  $\hat{\Lambda}_{GLRT\text{-multi}} (7 \times 7)$ . Bottom:  
 $\hat{\Lambda}_{GLRT\text{-mono}} (5 \times 5)$ .

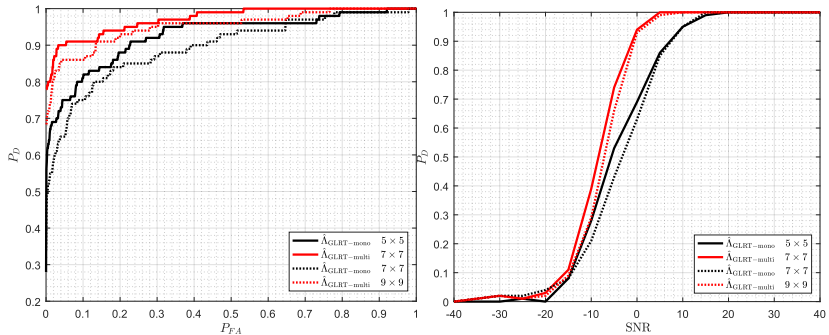


**Figure:** Left:  $P_D = f(P_{FA})$  computed on 100 Monte-Carlo trials (SNR =  $-5$ dB,  $N_k = N_\theta = 5$ , random position of the target and random steering vector). Right:  $P_D = f(\text{SNR})$  computed on 100 Monte-Carlo trials ( $P_{FA} = 10^{-3}$ ,  $N_k = N_\theta = 5$ , random position of the target and random steering vector).

## Conclusions

- Time-Frequency Analysis can be applied successfully on full-resolution mono-channel complex SAR images to exploit physical diversities such as frequency and angular behaviors of the pixels.
- This methodology allows to characterize a vector of information for each pixel of the SAR image. This vector of information can be used through Adaptive Detectors schemes to detect both bright scatterers and anisotropic and colored target.
- Merging this Time-Frequency approach with robust detection schemes (ANMF and Tyler's M-estimator) may lead to a good improvement in terms of detection performance and particularly in terms of False Alarm regulation when dealing with heterogeneous and non-Gaussian SAR images,
- Change Detection problematic using this diversity has been explored and shows promising results.

## Perspectives

- The approach can be extended to Polarimetric images.
- Change detection using CES modelling will be explored.
- Time Series of images : how to derive a test using the covariance matrices ?

